Synthetic Metals, 62 (1994) 187–192

A photoemission study of *c*-axis-oriented thin films of α-(BEDT–TTF)$_2$I$_3$

S. Söderholm and B. Loppinet

Materials Physics, Department of Physics, Royal Institute of Technology, S-100 44 Stockholm (Sweden)

D. Schweitzer

3. Physikalisches Institut, Universitat Stuttgart, Pfaffenwaldring 57, D-70550 Stuttgart (Germany)

(Received October 5, 1993; accepted November 9, 1993)

Abstract

Highly *c*-axis-oriented thin films of α-(BEDT–TTF)$_2$I$_3$ have been prepared by physical vapour deposition. Structural and morphological characterization are performed by X-ray diffraction and scanning electron microscopy. *In situ* photoemission experiments on the films reveal five distinct features in the valence-band regime; the two structures with the lowest binding energies are assigned to molecular orbitals present in the TTF backbone. None of the valence-band structures shows dispersion along the Γ-Z (k_z) direction. The spectral intensity is zero at, and to within 0.5 eV of the Fermi level. Core-level spectroscopy on the I 4d level indicates that all iodine is present as I_3^- ions and that the surface consists of BEDT–TTF molecules.

1. Introduction

Since the discovery of the first organic conductor, TTF–TCNQ, in 1973 [1], there has been great interest amongst physicists and chemists in organic conductors. Research in this field was further stimulated when the first organic superconductor (TMTSF)$_2$PF$_6$ (T_c=0.9 K, p=12 kbar) was reported in 1980 [2]. In 1983 the first sulfur–containing ambient-pressure superconductor, β-(BEDT–TTF)$_2$I$_3$ (T_c=1.4 K), was synthesized [3]. BEDT–TTF is an abbreviation for bis(ethylenedithio)–tetrathiafulvalene; its molecular structure is shown in Fig. 1. A majority of the organic superconductors known today are based on BEDT–TTF with κ-(BEDT–TTF)$_2$Cu[N(CN)$_2$]Br having the highest critical temperature at ambient pressure, T_c=11.6 K [4]. The salts of BEDT–TTF appear in many crystallographic phases and have widely different properties. Generally the BEDT–TTF salts have a layered structure consisting of alternating layers of conducting BEDT–TTF molecules and of anions. This layered structure causes the electronic structure to be two dimensional. Even if many BEDT–TTF salts have been thoroughly studied, some fundamental questions are still unanswered, among them: the mechanism behind the superconductivity, and the way in which the crystal structure influences the electronic structure, e.g., why has β-(BEDT–TTF)$_2$I$_3$ a superconducting ground state while α-(BEDT–TTF)$_2$I$_3$ shows a metal–insulator transition at 135 K [5]?

One way to get additional information on these materials is by means of photoelectron spectroscopy, but this kind of experiment has been hampered by the difficulties in obtaining surfaces clean enough for this surface-sensitive technique. However, the possibility of preparing thin films of α- and β-(BEDT–TTF)$_2$I$_3$ by evaporation [6] has made it possible to circumvent this problem.

In this communication the preparation and characterization by scanning electron microscopy (SEM) and X-ray diffraction of *c*-axis-oriented thin films of α-(BEDT–TTF)$_2$I$_3$ and *in situ* photoemission experiments on these films are reported.

2. Experimental

The *c*-axis-oriented thin films of α-(BEDT–TTF)$_2$I$_3$ were prepared by physical vapour deposition (PVD), essentially as described by Kawabata *et al.* [6]. In order to facilitate *in situ* measurements, the PVD was performed in a custom-made preparation chamber attached to the analysis chamber on the beam line. The raw material was obtained by grinding electrochemically prepared (BEDT–TTF)$_2$I$_3$ crystals, in most cases of the α-phase. The stainless steel crucible was resistively heated. The substrate was heated by radiation from a halogen–tungsten lamp. The temperature of the crucible

SSDI 0379-6779(93)02038-M

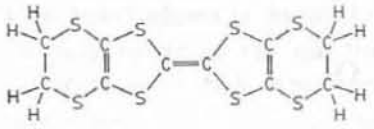

(a)

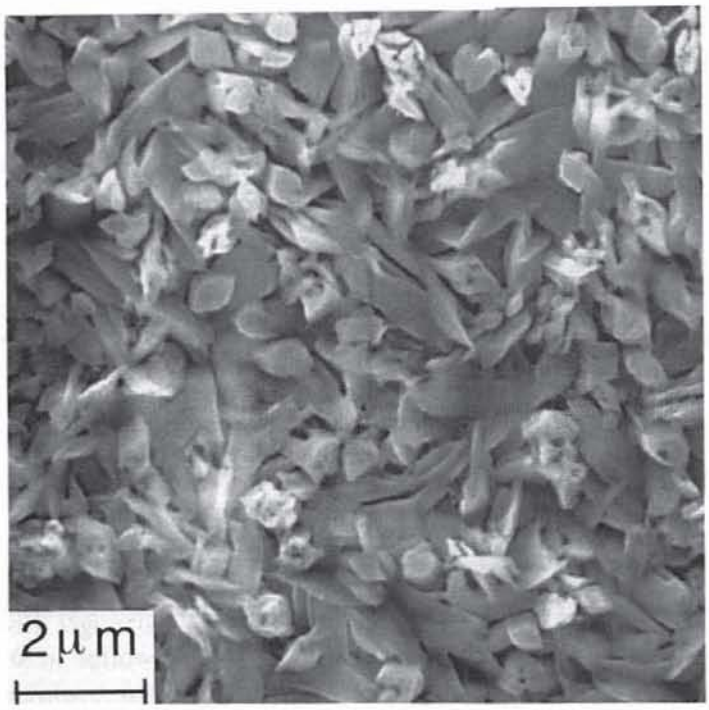

(b)

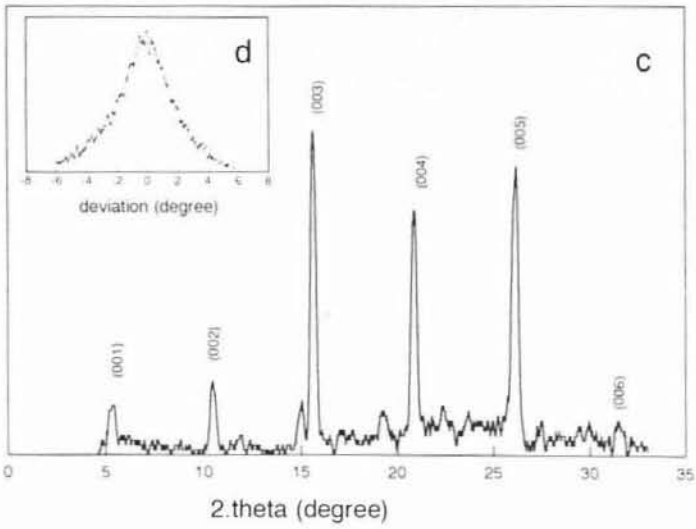

Fig. 1. (a) Molecular structure of BEDT–TTF [bis(ethylenedithio)–tetrathiafulvalene]. (b) SEM image of an α-(BEDT–TTF)$_2$I$_3$ film grown on a stainless-steel substrate (T_s = 70 °C). (c) A Θ–2Θ X-ray diffraction scan of an α-(BEDT–TTF)$_2$I$_3$ film on a glass substrate. (d) Rocking curve measured on the (005) peak of the film in (c).

and the substrate were monitored with Pt100 resistors. During the PVD the distance between the crucible and the substrate was around 30 mm and when the substrate temperature was 70 °C, α-(BEDT–TTF)$_2$I$_3$ was obtained. The pressure was maintained at 10^{-5} mbar during the evaporation, the base pressure in the preparation chamber being around 5×10^{-8} mbar.

The films were prepared on two kinds of substrates; stainless steel for the photoemission experiments and SEM, and on glass for the characterization by SEM, X-ray diffraction and infrared spectroscopy.

The photoemission experiments were performed on beamline 41 at the MAX Synchrotron Radiation Laboratory in Lund, Sweden. The spectra were recorded with a goniometer-mounted modified VSW hemispherical angle resolving electron energy analyser; for a comprehensive description of the beamline, see Karlsson *et al.* [7]. The total energy resolution, photon and electron contributions, was determined from the Fermi edge of thoroughly sputtered stainless steel, i.e., part of the sample holder, to be 0.25 eV at a photon energy of 20 eV and 0.40 eV at 150 eV. The base pressure in the analysis chamber was about 5×10^{-10} mbar.

3. Results and discussion

The crystallographic structure has been investigated for the films on a glass substrate by X-ray diffraction with Cu Kα radiation. The spectrum (see Fig. 1(c)) shows a reflection at $2\theta = 5.22°$ and higher orders of this reflection that fit the $\langle 00l \rangle$ family of α-(BEDT–TTF)$_2$I$_3$. The presence of only strong lines belonging to $\langle 00l \rangle$ shows that the film is highly oriented with the c-axis perpendicular to the substrate. The c-axis orientation is further proved by the rocking curve of the (005) peak (Fig. 1(d)). The full width at half maximum is 3.61°, in other words, approximately 45% of the crystallites are oriented within 5°. The SEM images of the films on glass and on stainless-steel substrates are essentially the same. The crystallites were found to be roughly 1–2 μm large in both cases, and show the plate-like morphology of α-(BEDT–TTF)$_2$I$_3$ single crystals (see Fig. 1). A SEM image also reveals that a c-axis orientation is preferred.

Figure 2 shows photoemission spectra of an α-(BEDT–TTF)$_2$I$_3$ film obtained in normal emission with different photon energies in the range 40–150 eV. Five distinct structures can be observed in the valence-band regime. These structures cover the binding-energy range 0.5–11 eV relative to the Fermi level $E_F = 0$. In this Figure two shallow core levels (inner valence states) at $E_b = 13.9$ eV and $E_b = 18.1$ eV are also seen. These structures cannot unambiguously be assigned to certain levels, since it is not clear to what extent these orbitals mix with the valence band (or if they are a part of the valence band). However, there is no contribution from iodine to the spectral intensity in the regime around the shallow core levels. This conclusion is based on studies of films found to be iodine deficient.

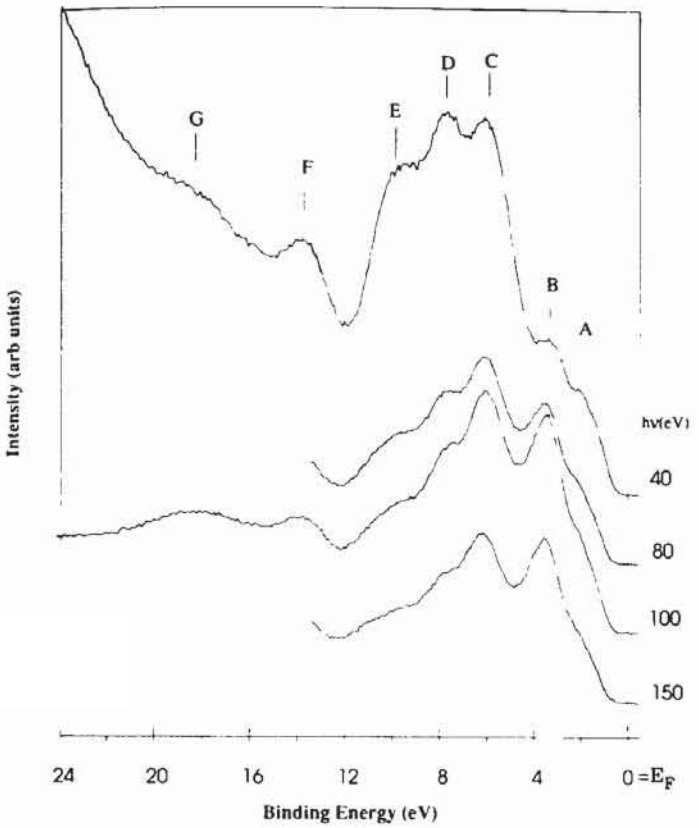

Fig. 2. Photoemission spectrum of an α-(BEDT–TTF)$_2$I$_3$ film obtained in normal emission with photon energies between 40 and 150 eV, showing the valence band. The labels A to E indicate different structures in the valence-band regime, and F and G indicate two shallow core levels (inner valence states).

A comparison of the normal emission valence-band spectra obtained with different photon energies shows that none of the bands, labelled A–E in Fig. 2, is dispersing in the Γ-Z (k_z) direction. This is in agreement with the two-dimensional electronic structure of the BEDT–TTF salts deduced from galvanometric measurements [8]. Since the spectra in Fig. 2 are normalized to the photon flux, it is clear that not only the relative intensities of the features in the valence band but also the probability for electron emission are strongly dependent on the energy of the excitation radiation. These spectra also show that there is no emission at the Fermi level along the Γ-Z line in the Brillouin zone, the spectral intensity being zero to within 0.5 eV below E_F.

The origin of some of these features can be deduced, since for many organic compounds the photoemission spectra of the gas phase and the solid are similar, the bands in the spectrum of the solid being broadened and rigidly shifted [9–11]. This indicates that the molecular orbitals dominate the bands of the solid, and are relatively unaffected by the solidification. Moreover, even in the case of charge-transfer (CT) complexes, the features in the valence band can be traced back to bands in the gas-phase spectra [12], implying that the electronic structure of the CT complex is governed by the electronic structure of the different molecules forming the solid. Through a comparison of the gas-phase spectra of TTF [13, 14], TTMTTF (tetrathiomethoxytetrathiafulvalene) [15] and BEDT–TTF [15], with the spectrum of α-(BEDT–TTF)$_2$I$_3$ (see Fig. 3), some information on the origin of the bands can be obtained. (TTMTTF can be regarded as the link between TTF and BEDT–TTF, with respect to the molecular structure.)

With the aid of Fig. 3, structures A and B in the spectrum of α-(BEDT–TTF)$_2$I$_3$ can be said to arise from the first and third molecular orbitals of BEDT–TTF with ionization potentials referred to the vacuum level of 6.5 and 7.8 eV, respectively. Structure C most likely arises from a combination of the three orbitals in BEDT–TTF with an ionization potential (I_g) around 10.5 eV, with the largest contribution from the strongest feature in the gas-phase spectrum at $I_g = 10.1$ eV. The peaks D and E can be traced back to multitudes of unresolved structures in the BEDT–TTF gas-phase spectrum around 12 and above 13 eV, respectively. It is interesting that no traces of the BEDT–TTF orbital at $I_g = 7.2$ eV nor from the orbitals around 9 eV can be seen in the spectrum of α-(BEDT–TTF)$_2$I$_3$. This is probably not due to the broadening of the structures occurring upon solidification, since if the structures in the BEDT–TTF spectrum giving rise to B and C were broadened so much that structures corresponding to $I_g \approx 9$ eV became obscured, it is very unlikely that B and C should be as well resolved as they are. Furthermore, no additional structures become resolved in the spectrum of α-(BEDT–TTF)$_2$I$_3$ when the intensity

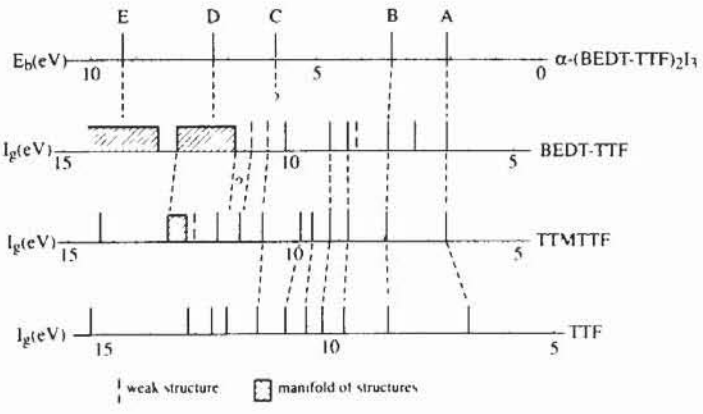

Fig. 3. Schematic representation of the photoemission spectrum of (from bottom up) TTF gas phase, TTMTTF gas phase, BEDT–TTF gas phase, and an α-(BEDT–TTF)$_2$I$_3$ film. The bars represent structures in the different spectra; weak ones are indicated by broken bars, and the hatched areas represent manifolds of unresolved/poorly resolved structures. Dotted lines give the tentative correspondence between features in different spectra. The spectra are aligned to give the best coincidence. The energy scale of the gas-phase spectra is the ionization potential with respect to the vacuum level. The gas-phase data are from refs. 13–15.

of B is reduced, i.e., when the photon energy is decreased, see Fig. 2.

Other ways of aligning the spectra, for instance by neglecting the orbital with $I_g = 6.5$ eV, a weak structure according to Sato *et al.* [15], give the same result; the lack of structures between A and B, and/or B and C cannot be explained satisfactorily only by broadening of the orbitals upon solidification.

The correspondence of structures in the gas-phase spectra of TTF, TTMTTF and BEDT–TTF with the proposed alignment of the spectra (Fig. 3) indicates that the bands in α-(BEDT–TTF)$_2$I$_3$ with the lowest binding energy are formed by molecular orbitals present in the TTF backbone of the BEDT–TTF molecule. These orbitals in TTF are those with the lowest I_g (see Fig. 3), and have been assigned to π-orbitals [14].

The valence-band spectrum of iodine-deficient samples, i.e., those in which the I 4d signal was very weak, showed the same structures A–E, but the spectral intensities of A and B were very low and structure E was enhanced. The former suggests that the I 5p density of states is rather high in this regime. But the lack of a shift of the binding energies indicates that the hybridization between I 5p and C 2p/S 3p is very small.

The lack of spectral intensity at the Fermi edge most probably reflects the absence of a finite density of states at the Fermi level and is not related to the organic nature of α-(BEDT–TTF)$_2$I$_3$ or the compound's low-dimensional electronic structure. This is true even if earlier photoemission experiments on organic compounds with metallic properties, i.e., TTF–TCNQ and other TCNQ compounds, did not show any intensity at E_F [12, 16, 17]. This was explained by the excitations of high-energy phonons in the photoemission process, which should shift the emission to higher binding energies and broaden the spectral features [12]. A recent and comprehensive study by Dardel *et al.* [18] on metallic systems with different dimensionality showed that only one-dimensional systems lacked a Fermi edge. In the view of photoemission studies on one-dimensional radical anion salts of 2,5-substituted dicyanoquinodiimine (DCNQI) [19, 20], the most plausible explanation for the lack of a Fermi edge is interacting electrons. However, DCNQI salts whose electrical and magnetic properties are well explained by a narrow-gap semiconductor model, where the gap is due to correlation effects, showed an energy separation between the valence-band maximum and the Fermi level of the same order of magnitude as the energy gap obtained from electrical and magnetic measurements [19]. Thus, the lack of intensity at E_F for α-(BEDT–TTF)$_2$I$_3$* is a real feature independently of the assumed dimensionality of the electronic structure and/or the presence of correlation effects, since optical measurements show the presence of a small bandgap, roughly 50 meV [21].

Another reason for the presence of a bandgap is that the surface sensitivity of photoemission could cause the spectra to be dominated by the top layer of the film, which probably consists of BEDT–TTF (see below), and this layer could have an electronic structure different from the bulk structure. But if the surface does consist of a neutral BEDT–TTF film, the bandgap should be much larger than the deduced value.

However, the determined bandgap is in fair agreement with band-structure calculations of α-(BEDT–TTF)$_2$I$_3$ performed with the tight-binding scheme based upon the extended Hückel method [22, 23]. These calculations predict that α-(BEDT–TTF)$_2$I$_3$ is a narrow-gap semiconductor with a direct energy gap of 14 meV at the Y point [22]. Emge *et al.* [22] and Mori *et al.* [23] argue that the very narrow gap should give rise to the apparent metallic behaviour observed above the phase transition [5]. These calculations also predict that the four derived bands span a very narrow energy range of about 0.3 eV. The observed bandgap at the Γ point is in qualitative agreement with the calculations; depending on the number of excited charge carriers, the top of the valence band at Γ should be about 0.1–0.15 eV below E_F [22]. This discrepancy has two likely sources. The first is that correlation effects must be taken into account, which should increase the magnitude of the bandgap. It has been proposed from experimental data, mainly magnetic and optical measurements, that the bandwidth and the correlation effects are of the same magnitude [22–25]. The second is that the accuracy of the calculations is not good enough because of the simplifications introduced. A comparison between extended Hückel tight-binding calculations [23, 26] and a first-principle self-consistent-field method (the pseudofunction method) [27] for β-(BEDT–TTF)$_2$I$_3$ shows that the results of the calculations are in qualitative agreement, but the bandgaps and bandwidths are different.

The I 4d core level was also studied. From a fit to the experimental data, the binding energy for the $4d_{5/2}$ level was determined as 48.9 eV, and the spin–orbit split as 1.71 eV, see Fig. 4. The fitted lineshape in this Figure was obtained from the convolution of a Lorentzian line with a Gaussian line, in order to simulate the broadening of the spectrum due to the resolution of the apparatus, phonons and disorder. The full width at half maximum (FWHM) of the Lorentzian line, i.e., the lifetime of the core hole, was 0.20 eV, and the Gaussian line had a FWHM of 0.97 eV. The large width of the core-level peaks is probably mainly due to phonon broadening, since organic conductors are 'soft materials' in the sense that many phonons are

*D. Schmeisser (personal communication) has observed a finite $N(E_F)$, depending on the iodine pressure during the PVD. The structural information on these films is sparse.

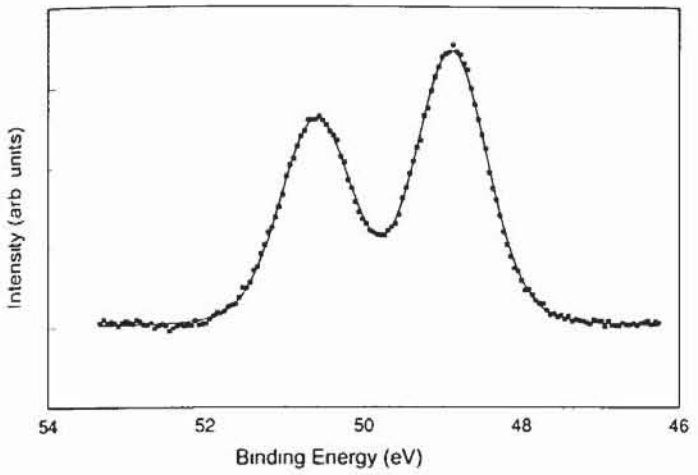

Fig. 4. I 4d core-level spectrum, excited with a photon energy of 100 eV. The squares represent the experimental points. The full line is a calculation, and the parameters used in the calculation are given in the text.

excited at room temperature, as seen for instance by the large thermal ellipsoids obtained in X-ray diffraction experiments. The I 4d spectrum recorded at an emission angle of 50° could be fitted with the same parameters. The fact that the only difference between the spectra recorded at different emission angles was the intensity and that the spectra could be fitted with only one line indicates that all iodine is present as I_3^- ions.

Furthermore, the normal emission and the 50° emission spectrum being congruent implies that no I_3^- ions are situated close to or at the surface, the *a–b* plane, since no surface-shifted component could be detected. This implication is consistent with scanning tunnelling microscopy on α- [28] and β-(BEDT–TTF)$_2$I$_3$ [29], which reveals no iodine on the surface of the crystals; a reconstruction was observed on the surface of β-(BEDT–TTF)$_2$I$_3$, which has been attributed to the instability of the anion layer [29].

4. Conclusions

Thin films of the organic conductor α-(BEDT–TTF)$_2$I$_3$ have been prepared by physical vapour deposition. Structural and morphological characterizations were performed by X-ray diffraction and scanning electron microscopy. The former method showed that the films were highly *c*-axis oriented, about 45% of the crystallites being oriented within 5°. Images obtained with scanning electron microscopy show that the crystallites have the same plate-like morphology as single crystals and have a size of about 1–2 μm.

In situ photoemission experiments on the films revealed five distinct structures in the valence-band regime, 0.5–11 eV below the Fermi level. The structures with the lowest binding energies are assigned to molecular orbitals present in the TTF backbone. Angular resolved measurements showed no dispersion along the Γ-Z (k_z) direction for the structures in the valence-band regime. The spectral intensity was found to be zero down to 0.5 eV below the Fermi level.

Core-level spectroscopy on the I 4d level indicated that all iodine is present as I_3^- ions, and that no such ions are situated close to or at the surface, the *a–b* plane, i.e., the surface consists of BEDT–TTF molecules.

Acknowledgements

The authors are very grateful for the skilful help given by L. Thånell and N. Persson, MAX-lab, with the design and manufacture of the preparation chamber. Financial support from the Göran Gustafssons Foundation and the Swedish Natural Science Research Council is gratefully acknowledged.

References

1 J. Ferraris, D.O. Cowan, V.V. Walatka and J.H. Perlstein, *J. Am. Chem. Soc., 95* (1973) 948; L.B. Coleman, M.J. Cohen, D.J. Sandman, F.G. Yamagishi, A.F. Garito and A.J. Heeger, *Solid State Commun., 12* (1973) 1125.
2 D. Jérome, A. Mazaud, M. Ribault and K. Bechgaard, *J. Phys. Lett. (Paris), 41* (1980) L95.
3 E.B. Yagubskii, I.F. Shchegolev, V.N. Laukhin, P.A. Kononovich, M.V. Kartsovnic, A.V. Zvarykina and L.I. Bubarov, *JETP Lett., 39* (1984) 12.
4 A.M. Kini, U. Geiser, H.H. Wang, K.D. Carlson, J.M. Williams, W.K. Kwok, K.G. Vandervoort, J.E. Thompson, D.L. Stupka, D. Jung and M.-H. Whangbo, *Inorg. Chem., 29* (1990) 2555; J.M. Williams, A.M. Kini, H.H. Wang, K.D. Carlson, U. Geiser, L.K. Montgomery, G.J. Pyrka, D.M. Watkins, J.M. Kommers, S.J. Boryschuk, A.V. Strieby Crouch, W.K. Kwok, J.E. Schirber, D.L. Overmyer, D. Jung and M.-H. Whangbo, *Inorg. Chem., 29* (1990) 3272.
5 K. Bender, I. Hennig, D. Schweitzer, K. Dietz, H. Endres and H.J. Keller, *Mol. Cryst. Liq. Cryst., 107* (1984) 359; I. Hennig, K. Bender, D. Schweitzer, K. Dietz, H. Endres, H.J. Keller, A. Gleitz and H.W. Helberg, *Mol. Cryst. Liq. Cryst., 119* (1985) 337.
6 K. Kawabata, K. Tanaka and M. Mizutani, *Solid State Commun., 74* (1990) 83; K. Kawabata, K. Tanaka and M. Mizutani, *Synth. Met., 41–43* (1991) 2097.
7 U.O. Karlsson, J.N. Andersen, K. Hansen and R. Nyholm, *Nucl. Instrum. Methods A, 282* (1989) 553.
8 T. Ishiguro and K. Yamaji, *Organic Superconductors,* Springer, Berlin, 1990, pp. 99–147.
9 W.D. Grobman and E.E. Koch, in L. Ley and M. Cardona (eds.), *Photoemission in Solids,* Vol. 2, Springer, Berlin, 1979, pp. 261–298.
10 P. Nielsen, *Phys. Rev. B, 10* (1974) 1673.
11 N. Sato, H. Inokuchi and I. Shirotani, *Chem. Phys., 60* (1981) 327.
12 W.D. Grobman, R.A. Pollak, D.E. Eastman, E.T. Maas, Jr and B.A. Scott, *Phys. Rev. Lett., 32* (1974) 534.
13 R. Gleiter, E. Schmidt, D.O. Cowan and J.P. Ferraris, *J Electron Spectrosc. Rel. Phenomen., 2* (1973) 207.

14 A.J. Berlinsky, J.F. Carolan and L. Weiler, *Can. J. Chem., 52* (1974) 3373.
15 N. Sato, G. Saito and H. Inokuchi, *Chem. Phys., 76* (1983) 79.
16 P. Nielsen, A.J. Epstein and D.J. Sandman, *Solid State Commun., 15* (1974) 53.
17 P. Nielsen, D.J. Sandman and A.J. Epstein, *Solid State Commun., 17* (1975) 1067.
18 B. Dardel, D. Malterre, M. Grioni, P. Weibel, Y. Baer and F. Lévy, *Phys. Rev. Lett., 67* (1991) 3144.
19 D. Schmeisser, W. Göpel, U. Langohr, J.U. von Schütz and H.C. Wolf, *Synth. Met., 41–43* (1991) 1805.
20 D. Schmeisser, A. Gonzales, J.U. von Schütz, H. Wachtel and H.C. Wolf, *J. Phys. France I, 1* (1991) 1347.
21 V. Železný, J. Petzelt, R. Swietlik, B.P. Gorshunov, A.A. Volkov, G.V. Kozlov, D. Schweitzer and H.J. Keller, *J. Phys. France, 51* (1990) 869.
22 T.J. Emge, P.C.W. Leung, M.A. Beno, H.H. Wang, J.M. Williams, M.-H. Whangbo and M. Evain, *Mol. Cryst. Liq. Cryst., 138* (1986) 393.
23 T. Mori, A. Kobayashi, Y. Sasaki, H. Kobayashi, G. Saito and H. Inokuchi, *Chem. Lett.,* (1984) 957.
24 N. Toyota, E.W. Fenton, T. Sasaki and M. Tachiki, *Solid State Commun., 72* (1989) 859; N. Toyota and T. Sasaki, *Synth. Met., 41–43* (1991) 2235.
25 F.L. Pratt, J. Singleton, M. Kurmoo, S.J.R.M. Spermon, W. Hayes and P. Day, *Physics and Chemistry of Organic Superconductors, Proc. ISSP Int. Symp., Tokyo, Japan, Aug. 28–30, 1989,* Springer, Berlin, 1990, p. 200.
26 M.-H. Whangbo, J.M. Williams, P.C.W. Leung, M.A. Beno, T.J. Emge, H.H. Wang, K.D. Carlson and G.W. Crabtree, *J. Am. Chem. Soc., 107* (1985) 5815.
27 R.V. Kasowski and M.-H. Whangbo, *Inorg. Chem., 29* (1990) 360.
28 Y.F. Miura, A. Kasai, T. Nakamura, H. Komizu, M. Matsumoto and Y. Kawabata, *Mol. Cryst. Liq. Cryst., 196* (1991) 161.
29 M. Yoshimura, H. Shigekawa, H. Yamochi, G. Saito, Y. Saito and A. Kawazu, *Phys. Rev. B, 44* (1991) 1970.